

INTERNATIONAL SOCIETY FOR SOIL MECHANICS AND GEOTECHNICAL ENGINEERING



This paper was downloaded from the Online Library of the International Society for Soil Mechanics and Geotechnical Engineering (ISSMGE). The library is available here:

<https://www.issmge.org/publications/online-library>

This is an open-access database that archives thousands of papers published under the Auspices of the ISSMGE and maintained by the Innovation and Development Committee of ISSMGE.

Geosynthetic reinforced bearing layers for working platforms of mobile construction machines and cranes

Couches d'assise renforcées par géosynthétique pour platesformes de travail utilisées pour machines de construction mobiles et grues

R. Worbes, Ch. Moormann

Institute for Geotechnical Engineering – University of Stuttgart, Germany

ABSTRACT: For the installation of heavy mobile construction machines, such as rotary drilling devices, concrete pumps and heavy crawler cranes, temporary working platforms are often created in the form of filled and compacted earthworks reinforced with geogrids. These working platforms shall ensure a safe and usable setup of the construction machinery, taking all relevant loading conditions into account. The performed 1-g model tests presented in this paper simulate the loading from construction machines on reinforced bearing layers on weak subgrades under static and cyclic loading in the scale 1:3. In this context, different parameters of bearing layers such as the number of reinforcement layers, the tensile rigidity of the reinforcement and the undrained shear strength of the subgrade are varied.

RÉSUMÉ: Pour l'installation de machines de construction mobiles lourdes, telles que les foreuses rotatives, les pompes à béton et les grues sur chenilles lourdes, des plates-formes de travail temporaires sont souvent créées sous la forme de terrassements versés et compactés armés de géogrilles. Ces plates-formes de travail doivent assurer une installation sûre et utilisable des engins de construction, en tenant compte de tous les cas de charge pertinents. Les essais sur modèle réalisés à 1 g présentés dans cet article simulent le chargement des machines de construction sur des couches d'assise renforcées sur des sous-sols faibles soumis à des charges statiques et cycliques à l'échelle 1: 3. Dans ce contexte, les différents paramètres des couches d'appui, tels que le nombre de couches de renforcement, la rigidité de l'armature et la résistance au cisaillement non drainée du sol, sont variés.

Keywords: working platforms, bearing capacity, geogrid reinforcement, 1-g model tests

1 GUIDELINES

During the installation and operation of mobile construction machines, accidents and machine overturns occur again and again with corresponding considerable damage to property and personal injury. According to a study from the Building Research Establishment (2004), one third of all accidents involving construction machinery and cranes are caused by a

substandard underground. Affected is heavy mobile construction equipment such as rotary or trench wall devices, rams and all types of mobile and crawler cranes, but also lighter construction equipment such as mobile concrete pumps, elevators, etc. Figure 1 shows a current example of a crane accident on insufficient ground conditions, highlighting the serious consequences of such machine overturns. For the



Figure 1: crawler crane accident caused by insufficient ground conditions (www.simscrane.com)

use of mobile construction machines on soft ground often temporary working platforms in the form of filled and compacted, partially reinforced with geogrids earthworks are created. These working platforms have to ensure safe installation and operation of the construction machinery, taking into account all relevant operating and load conditions during their lifetime. They are therefore of central importance for occupational safety when using mobile construction machinery and cranes. In this context, there is an urgent need for improvement and optimization since on one hand the machine specific requirements often do not correlate with the prepared working platforms on site and, on the other hand there are no generally accepted design approaches available for dimensioning of temporary working platforms.

2 LOAD-BEARING MECHANISMS

The load-bearing behaviour of geosynthetic reinforced aggregate layers under static and non-monotonous loading conditions is characterized by several interaction mechanisms between the geosynthetic, the aggregate layer and the subgrade. There are four different load-bearing mechanisms discussed in literature, which can be identified for increasing the overall bearing capacity and durability of base course systems [Bender &

Barnberg (1978), Giroud & Bonaparte (1984), Perkins & Ismeik (1997), Koerner (2012)].

2.1 Lateral restraint

Load spreading as a result from vertical loading induces additional lateral stresses in the aggregate layer directly under the load plate. An unreinforced aggregate layer has practically no tensile strength, so that the aggregate layer tends to deform laterally, unless it is restrained by the cohesion of the weak subgrade. The lateral stresses lead in unreinforced systems to horizontal displacement and deteriorate the aggregate layer by increasing the void ratio and reducing the thickness of the aggregate. Using geosynthetic reinforcements made from geotextiles or geogrids placed inside the aggregate layer or at the interface to the subgrade are able to transfer the lateral stress by frictional interaction and interlocking of the gravel inside the geogrid apertures. This additional lateral restraint increases the mean stress and acts like a confinement of the aggregates under the load area, what reduces horizontal displacements and the associated thickness and stiffness reduction of the aggregate layer.

2.2 Increased bearing capacity

Another effect is the influence of geosynthetic reinforcements on the shape of the shear surface in the soil body. Once shear failure of the supporting layer occurs, the load plate and underlying aggregates sink into the weak subgrade. The shear surface attempts to pass through the reinforcement, but if the geogrid has sufficient tensile strength this is not possible. Therefore plastic deformation occurs and the shear failure is shifted deeper to the weak subgrade, with some load being carried by the geogrid reinforcement. If the load increases, collapse will occur due to excessive deformation (punching shear failure) or rupture of the geogrid.

2.3 Tensile membrane effect

The third load-bearing mechanism assumes the geosynthetic acting as a tensile membrane. This effect results from vertical displacements of the aggregate layer beneath the load plate, what leads to a wave shaped deflection and an additional vertical component of the tensile force in the reinforcement and thus to an increase of the bearing capacity of the whole system. This effect requires a minimum of plastic deformation to take place and increases with additional settlements until the ultimate tensile strength in the reinforcement is reached and rupture occurs. The tensile membrane effect transfers the vertical stress to areas outside the assumed load spread angle. Additional vertical stress on the subsoil in the side areas increases the bearing capacity of the subsoil itself, due to higher vertical stress on the passive failure wedge.

2.4 Mattressing effect

Another effect that increases bearing capacity is the mattressing effect, which is commonly known from geocell systems. This effect mainly occurs in high reinforced systems with multiple reinforcement layers and high stiffness. Due to the high reinforcement degree, aggregates will be fully confined in the spacing between the reinforcement layers. Combined with the tensile stiffness of the lower reinforcement layer, this leads to an increase of the bending stiffness of the aggregate layer.

2.5 Separation effect

For the case of weak subgrades, the geogrid reinforcement also acts as a separating layer to prevent penetration of the aggregates into the weak soil on one hand and migration on fines into the aggregate layer on the other hand. This migration results from pumping effects and leads to reduced shear parameters of the aggregates due to the increased fines content. Pumping effects intensify under non-monotonous loading conditions (cyclic, dynamic).

3 MODEL TESTING

Using geotechnical model tests, allows to obtain deepened soil mechanic findings of the loadbearing and deformation behaviour of unreinforced and reinforced supporting layers on weak subgrades with low stiffness, under static and cyclic loading conditions. Aim of the experimental test concept hereby is to investigate the failure mechanism (punching fracture and mobilized shear planes) of unreinforced and reinforced two-layer systems. In addition to clarifying the failure mechanisms, the serviceability states were also represented by realistic load assumptions, frequencies and load cycles of typical construction machines. Figure 2 illustrates the geometry and the arrangement of the measuring sensors of the experiment. The basal area of the test field is 4.82 m x 2.72 m, in which two model tests can be prepared at once and conducted separately from each other. Each test field has the dimensions 2.41 m x 2.72 m. The size of the load plate is 35 cm x 25 cm (L x B) and represents the outriggers of mobile construction machines. The vertical load is

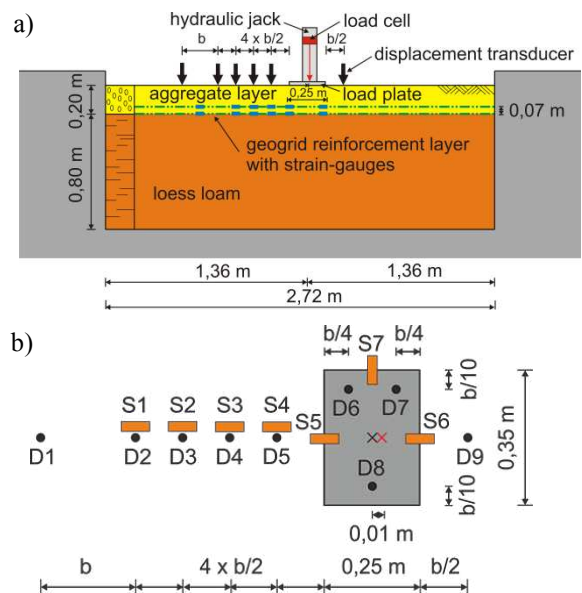


Figure 2: Setup and arrangement of the LVDTs and strain-gauge: a) cross section, b) Ground plan of load plate and measurement devices

applied with an eccentricity $e = 0.04 \cdot b = 1$ cm relative to the shorter plate side to control the direction of the ground failure. Deformations on the surface are measured by linear variable differential transformers (LVDT) at nine points. In the reinforced systems, the strains in the geogrids are measured at seven points by foil strain gauges.

3.1 Soils

The subgrade, represented by loess loam (SC/CL classification according to USCS) with an undrained shear strength c_u of 20 kN/m² with a thickness of 0.80 m. The soil parameters of the remoulded and compacted loess loam are controlled by the moisture content and the undrained shear strength measured by in-situ vane shear tests to ensure a constant quality. Above the soft layer, the aggregate layer is installed with a thickness of 0.20 m. For the installation of the bearing layer a well-graded sand-grit mixture with a grain size distribution between 0 mm and 16 mm is used (Figure 3). The aggregate is incorporated with the proctor density (compression factor $D_{Pr} = 100\%$).

3.2 Geosynthetics

In the unreinforced tests, a nonwoven is used as a separating element between subgrade and aggregate layer. It can be assumed that the

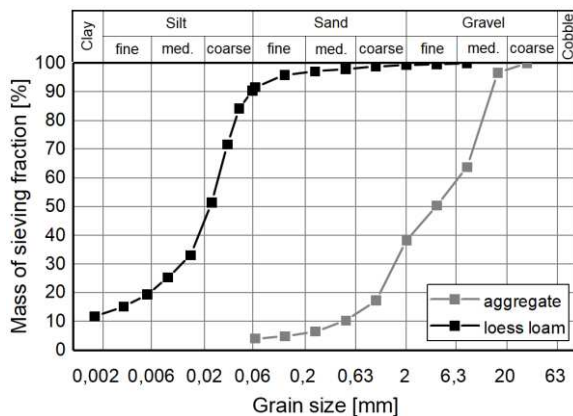


Figure 3: Grain-size distribution of sand-grit aggregate and loess loam

nonwoven geosynthetic membrane, has only a minor reinforcement function, which can be neglected. For the reinforced tests a composite product made of a biaxial geogrid (laid with welded knots) with a ultimate tensile strength of 30 kN/m and 60 kN/m and a nonwoven, which is also used in the unreinforced experiment, was used for the lower layer. The upper layer was reinforced with the same biaxial geogrid with a tensile strength of 30 kN/m.

3.3 Loading concept

The loading scheme, shown in Figure 4 can be divided into five different phases. The first stage MI is the monotonous loading phase, in which the vertical load is initially increased to the average cyclic load of 4.5 kN (64.3 kN/m²) with a velocity of 0.1 kN/s. This causes plastic deformations prior to the cyclic loading phase CI and provides information about the initial stiffness of the systems. After that the first cyclic loading phase CI, which simulates load effects under operating conditions, begins. In this phase 1.000 load cycles with a frequency of 0.1 Hz and an amplitude of 3.5 kN between 1 kN and 8 kN are applied. Subsequently follows the second stage with the monotonous phase MII, where the vertical load was increased to the average cyclic load of 11.5 kN (164.3 kN/m²) phase CII. In the second cyclic load phase CII another 1.000 load cycles with the same frequency and amplitude are applied between 11.5 kN and 18.5 kN. During the

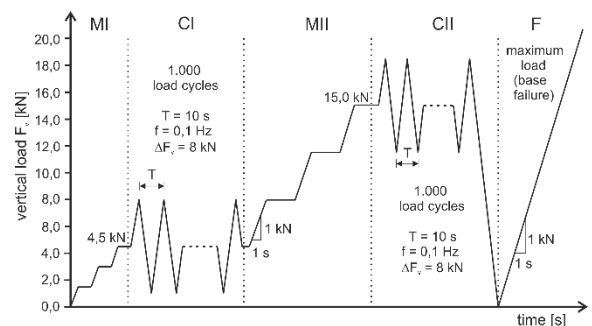


Figure 4: Loading concept with monotonous, cyclic and final loading phases (without technically necessary unloading phases)

final stage F, the load is increased up to a defined failure state, in order to obtain the ultimate bearing capacity.

Table 1: Testing matrix with properties

Test	Description	Subgrade strength c_u	Reinforcement arrangement
UR	Unreinforced granular base course	20 kN/m ²	None (non-woven for separation)
SR	Single layer reinforced base course	20 kN/m ²	biaxial geogrid $T_d = 30$ kN/m
DR	Double layer reinforced base course	20 kN/m ²	biaxial Geogrid 2x $T_d = 30$ kN/m
DR-HS	Double layer reinforced base course with high stiffness in the lower layer	20 kN/m ²	biaxial Geogrid $T_d = 30$ kN/m $T_d = 60$ kN/m

and 98% higher bearing capacities in comparison to the unreinforced system. The reinforcement degrees of these systems increases about 100% and 150% compared to system SR. As the tensile stiffness and thus the tensile strength of the geogrid reinforcement increases, a significant increase in bearing capacity, system rigidity and cyclic accumulation reduction can be observed. In this case, double layered reinforced systems show a disproportionately better performance compared to the higher reinforcement effort. The arrangement of the stiffer reinforcement in the lower layer in test DR-HS shows overall the best performance of the compared systems. Rupture of the geogrid reinforcement was observed in all tests except DR-HS and is the reason for system failure at lower settlements in test SR and DR. Especially in tests with uniform distribution of stiffness in both reinforcement layers, an early rupture of the lower layer induces to total system failure, although the reserves of the upper reinforcement layer are still hardly utilized.

4 MODEL TEST RESULTS

In the following the results of the four model tests (Table 2) with varied reinforcement arrangement UR (unreinforced), SR (single layer reinforcement), DR (double layer reinforcement) and DR-HS (double layer reinforcement with increased tensile stiffness of the lower reinforcement layer) are shown. All tests were conducted with same undrained shear strength $c_u = 20$ kN/m² of the subgrade and aggregate layer thickness $H = 20$ cm.

4.1 Bearing capacity

The load settlement curves in Figure 5 show the influence of the geogrid reinforcement on the system rigidity and bearing capacity. The deformational performance of the single reinforced system SR shows for 100 mm settlement about 20% and the double layered reinforced systems DR and DR-HS about 43%

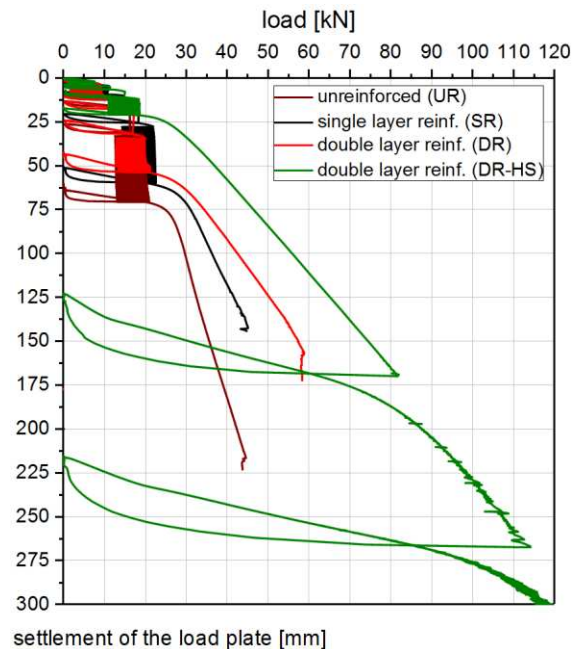


Figure 5: settlement of the load plate for different bearing layer systems

Settlement accumulation in the 1st cyclic loading phase

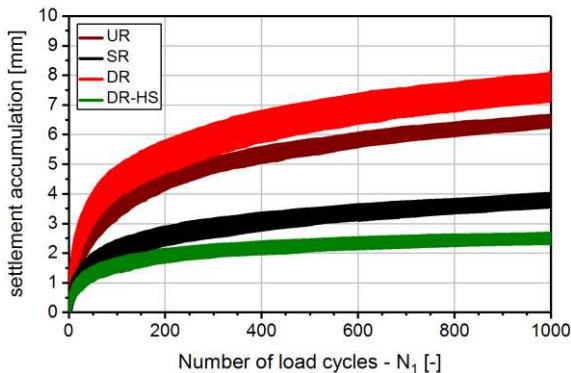


Figure 6: settlement accumulation of phase CI

4.2 Cyclic loading

Figure 6 and 7 shows the vertical deformation accumulation of the load plate during the cyclic loading phases CI and CII. Obviously, all systems initially deform more strongly in the first 50 – 100 load cycles. In phase CI the Systems lowest settlement accumulation after 1.000 cycles was observed for the system DR-HS with about 2,5 mm, followed by the single layered system DR with 3,75 mm and the unreinforced system UR with 6,25 mm. Test DR shows in phase CI the highest permanent deformation accumulation and greater deformations intervals for each load cycle, and therefore a larger elastic deformation region. This might be a consequence of the low influence of the geogrid reinforcement for small deformation and the negative influence of the upper geogrid layers on the compaction of the aggregates. In the second cyclic loading phase CII the settlement accumulation is graded according to the degree of reinforcement, due to the activation of the geogrid reinforcement what leads to plastic deformation reduction with increased reinforcement degree. The reinforcement benefit in Figure 7 is approx. proportional to the reinforcement degree of the base course systems.

Settlement accumulation in the 2nd cyclic loading phase

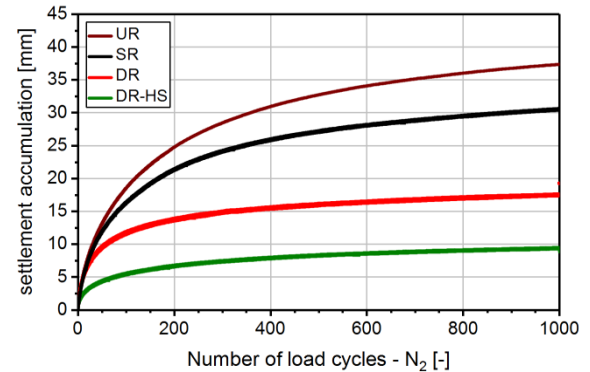


Figure 7: settlement accumulation of phase CII

4.3 Surface deformation

The surface deformations along the measuring axis from Sensor D1 to D9 (see Figure 2b) is shown in Figure 8 for the final settlement after the cyclic loading phases CI and CII as well for 30 kN and 40 kN to compare the deformation behaviour of the systems UR, SR, DR and DR-HS. The unreinforced system UR shows for all load conditions the highest settlements and the subsidence cavity with the steepest flanks. The single reinforced system SR and the double layered system DR and DR-HS show significant lower settlements for higher load levels. For double reinforced systems DR and DR-HS the subsidence area is much wider and heavings occur in the peripheral area at sensor D1 to D3. This effect is most pronounced for test DR at 30 kN and 40 kN through the larger settlement and thus the stronger soil displacement. The heavings of the surface are an indicator for volume constant soil displacement in the weak subgrade and marks the sphere of the passive failure wedge at the surface. The failure mechanism hereby shows similarities with the local shear failure mode, while the unreinforced and single reinforced systems are more similar to the punching shear failure mode.

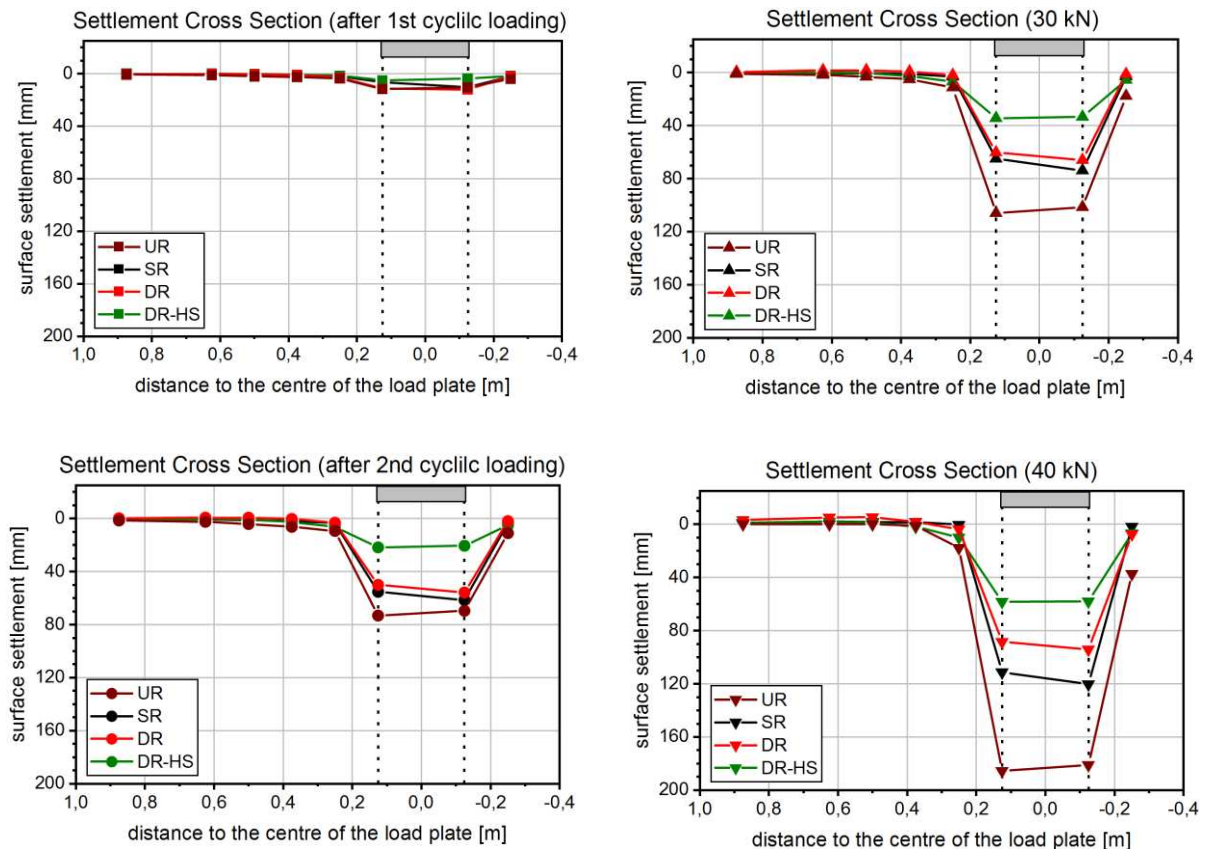


Figure 8: Surface settlements after the cyclic loading phases CI, CII and 30 kN and 40 kN of the final loading phase F

4.4 Reinforcement strain

The measured strains in the geogrid reinforcement layers of the systems SR, DR and DR-HS along the measurement axis from strain gauge S1 to S6 are shown for different loading conditions in Figure 9. Compared for each load level system SR shows a stronger strain development in the lower layer and thus faster activation of the geogrid reinforcement, than the double layered systems DR and DR-HS. One reason is the larger settlements of the system SR and by that a higher contribution of the tensile membrane effect. The strain levels in systems DR and DR-HS reach only 40 % resp. 17 % for 30 kN and 60 % resp. 25 % for 40 kN of the strain level of system SR. A comparison of the mobilized

strains in the upper and lower geogrid layer shows different distributions. While the lower layer has an increasing strain concentration under the load plate due to the increasing tensile membrane effect, the strains in the upper layer are significantly lower under the load plate and the other way round in the peripheral area. This results from the less favorable anchoring of the upper reinforcement layer in the base due to the low coverage and deflection. In the lower reinforcement layer the rate of change of strains, assuming an approximately linear relationship of geogrid stress and strain, indicates major changes in the normal force of the reinforcement and thus the shear stresses at the interface between the geogrid and subgrade resp. aggregate. This results, on one hand, from the lateral restraint and confinement of the base layer and, on the other

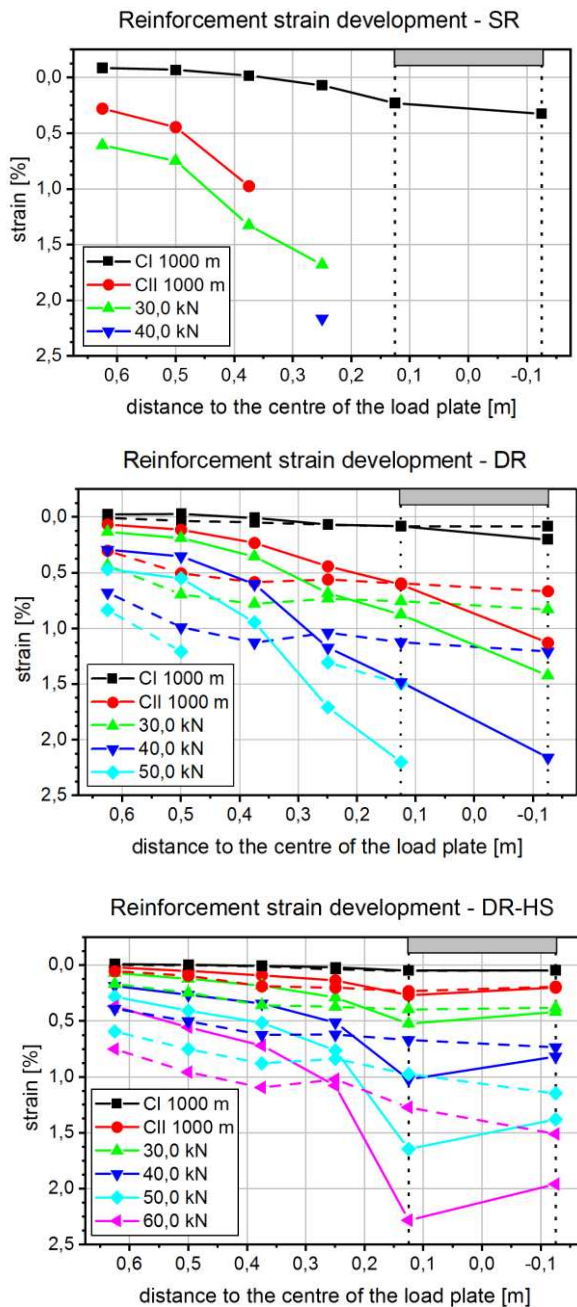


Figure 9: strain development in the reinforcement for model tests SR, DR and DR-HS

hand, from the tensile membrane effect. The tensile membrane effect transfers vertical stress and thus also shear strains to the subgrade in the area beside (1·B) the load plate.

5 CONCLUSIONS

The comparison of the model tests with different bearing layer systems for working platforms shows, that the load-deformation performance can be significantly optimised with geogrid reinforcements. The total bearing capacity and the system rigidity are increased for monotonous and cyclic loading conditions. Especially double reinforced systems with increased stiffness in lower reinforcement layer show high a improvement potential compared with unreinforced layers. The strain distribution for double reinforced layers indicates different bearing mechanisms for both reinforcement layers and a not inconsiderable contribution of the upper reinforcement layer especially for cyclic loading.

6 REFERENCES

- Bender, D.A. & Barnberg, E.J. 1978. Design of soil-fabric-aggregate system. Transportation Research Record 671, pp. 64-75.
- BRE - Building Research Establishment 2004/2007. Working platforms for tracked plant: good practice guide to the design, installation, maintenance and repair of ground-supported working platforms (BR 470). IHS BRE Press, Bracknell, Berkshire, ISBN 186081 7009.
- Giroud, J.-P., Ah-Line, C., and Bonaparte, R. 1984. Design of unpaved roads and trafficked areas with geogrids. Polymer Grid Reinforcement, A conference sponsored by SERC and Netlon, Ltd., Thomas Telford, London, England, pp. 116-127.
- Koerner, R.M. 2012. Designing with Geosynthetics, 6th Edition, New Jersey, Pearson Prentice Hall, Upper Sadle River.
- Perkins, S.W. & Ismeik, M. 1997. A Synthesis and Evaluation of Geosynthetic-reinforced Base Course Layers in Flexible Pavements: Part I + 2 Experimental Work. Geosynthetics International, Vol. 4, No. 6, pp. 549-621.